KSME International Journal, Vol. 13, No. 11, pp. 851~863, 1999

Low Reynolds Number k-ε Modeling with Improved ε Equation

Kyoung Song*, Geun Jong Yoo and Kang Rae Cho***

(Received March 19, 1999)

A series of k-ε model modification has been carried out using DNS data to include near wall effects. Though these methods aided by DNS data open new ways of turbulence modeling, the k-ε turbulence models still have shortcomings in predicting turbulent flows for various Reynolds numbers and various geometric conditions. Therefore a new k-ε models with improved dissipation rate of turbulent kinetic energy equation and the damping function for eddy viscosity model is proposed. The new dissipation rate equation is based on the energy spectrum and magnitude analysis. The damping function for eddy viscosity is also based on the dissipation rate length scale distribution near the wall and the DNS data. The new k-ε model is applied to fully developed turbulent flows in channels and pipes with a various Reynolds numbers. Predictions show that the proposed model represents properly the turbulence properties in all turbulent regions over a wide range of Reynolds numbers.

Key words : Low Reynolds Number, k-ε Model, Dissipation Rate, Energy Spectrum, Magnitude Analysis, Length Scale, Reynolds Number Effect, Damping Function

Nomenclature

C_ϕ : Model constants
D_k, D_ε : Molecular diffusion terms of k and ε equations, respectively
f_μ, f_β, f_ε : Damping functions
f_{Re} : Damping function for Re_δ effect
k : Turbulent kinetic energy ($k^+=k/u_\tau^2$)
P_k : Production term of k equation
$P_{\varepsilon 1}$: Mixed production term of ε equation
$P_{\varepsilon 2}$: Production term by mean velocity gradient in ε equation
$P_{\varepsilon 3}$: Gradient production term of ε equation
$P_{\varepsilon 4}$: Turbulent production term of ε equation
Re_t : Turbulent Reynolds number ($=k^2/\nu\varepsilon$)
Re_δ : Reynolds number based on mean flow velocity ($=U\delta/\nu$)
Re_τ : Reynolds number based on wall friction velocity ($=u_\tau\delta/\nu$)
S : Mean strain rate ($=dU/dy$)
T_k, T_ε : Turbulent diffusion terms of k and ε equation, respectively
U : Streamwise mean velocity ($U^+=U/u_\tau$)
u_i : Fluctuating velocity component
$\overline{u_iu_j}$: Turbulent shear stress ($\overline{u_iu_j}^+=\overline{u_iu_j}/u_\tau^2$)
u_τ : Wall friction velocity ($=\sqrt{\tau_w/\rho}$)
y^+ : Nomarlized wall distance ($=u_\tau y/\nu$)
Γ : Destruction term of ε equation
β : Ratio of mean field time scale to turbulent field time scale ($=S/(\varepsilon/\nu)^{1/2}$)
ε : Dissipation rate of k
$\tilde{\varepsilon}$: Psuedo dissipation rate of k ($=\varepsilon-2\nu(\sqrt{k}_{,j})^2$)
ν_t : Turbulent viscosity
ξ : Additional destruction term of ε equation
Π_k, Π_ε : Pressure diffusion terms of k and ε equation, respectively
σ_k, σ_ε : Turbulent Prandtl number
$\phi_{,i}$, $\phi_{,ii}$: First and second partial derivative with respect to x_i

* Department of Mechanical Engineering, Yonsei University, Seoul, Korea.
** Department of Mechanical Design and Manufacturing Engineering, Changwon National University, Changwon, Kyungnam, Korea.

$\bar{\phi}$: Time average of ϕ

1. Introduction

Turbulent flows are common in engineering. Therefore, various ways of the prediction for turbulent flow have been suggested, and turbulence modeling is a well known approach. Despite its shortcomings, turbulence modeling is widely applied to practical flows since its implementation is simpler than methods such as Direct Numerical Simulation (DNS). With this advantage, the main effort in turbulence modeling is focused on the accuracy improvement. Among many different types of turbulence models, the $k-\varepsilon$ model may be the most commonly used one. The standard $k-\varepsilon$ model is easy to use, but it is inadequate for complex flows due to its use of the wall function. Low Reynolds number $k-\varepsilon$ models (denoted by LRN hereafter) have been developed to eliminate the wall function from the standard $k-\varepsilon$ model. Jones and Launder(1972) initiated the LRN model development and Patel *et al.* (1985) studied performance of some LRN models. Hanjalic and Launder(1976) suggested a low Reynolds number turbulence model with an improved dissipation rate of turbulent kinetic energy equation model. Myong(1988) and Nagano and Tagawa(1990) also extended the LRN models, and their predictions show good agreement with the results of turbulent pipe flows of Laufer(1954). However, physical modeling of turbulent flows still contains inaccuracy to some degree.

DNS analyzes turbulent flows without physical modeling, and is widely accepted as a proper approach to obtain the detailed and accurate information of turbulent flow field. Turbulent channel flows of Mansour *et al.* (1988) and Kuroda *et al.* (1990) and turbulent flat plate boundary layer of Spalart(1988) are the examples of detailed DNS analyses. However, DNS requires huge computing capacity even for the simple turbulent flows. Therefore, the DNS results are more effectively utilized for validation of physical modeling rather than for flow field analysis itself. Rodi and Mansour(1993), Nagano and Shimada(1993), and Shin and Choi(1996) have proposed LRN models which are based on DNS data. Rodi and Mansour(1993) modified the equation of dissipation rate of turbulent kinetic energy and determined the damping function for turbulent viscosity by curve fitting DNS data. Nagano and Shimada(1993) improved Rodi and Mansour(1993)'s work further by including turbulent diffusion and pressure diffusion models in the dissipation rate equation. Shin and Choi (1996) modeled each term in the dissipation rate equation separately. These models generally show the good agreement with the DNS results for $Re_\tau=395$(Mansour *et al.*, 1988) on which their models were based. However, they show poor prediction ability for $Re_\tau=150$(Kuroda *et al.*, 1990). The models fail to reflect Reynolds number effects because the proposed models are based on curve fitting of DNS data at a particular Reynolds number without consideration of the near-wall behavior of turbulent properties.

In this study, a new LRN model is proposed utilizing DNS data. The proposed model includes an improved dissipation rate equation and an improved damping function for the turbulent viscosity. These are based on the distribution of turbulent properties near the wall without any fitted function. The proposed model also includes a method to account for the Reynolds number effect. This model is then applied to the fully developed channel and pipe flows of various Reynolds numbers. Prediction results are then compared with DNS data, and they show excellent agreement.

2. Turbulence Model

2.1 Governing equations

For incompressible, stationary turbulent flows, governing equations for mass, momentum and turbulent quantities can be written conveniently in Cartesian tensor notation as follows.

$$U_{i,i}=0 \tag{1}$$

$$\frac{DU_i}{Dt}=-\frac{1}{\rho}P_{,i}+\nu U_{i,jj}-(\overline{u_iu_j})_{,j} \tag{2}$$

The momentum Eq. (2), is not closed due to

$\overline{u_i u_j}$ terms and these terms are modeled with Boussinesq approximation and turbulent viscosity. The turbulent viscosity is given by Eq. (3), and the exact equation of the turbulent kinetic energy and its dissipation rate are given by Eqs. (4)-(5).

$$\nu_t = C_\mu f_\mu k^2/\varepsilon \tag{3}$$

$$\frac{Dk}{Dt} = P_k + T_k + \Pi_k + D_k - \varepsilon \tag{4}$$

$$\frac{D\varepsilon}{Dt} = P_{\varepsilon 1} + P_{\varepsilon 2} + P_{\varepsilon 3} + P_{\varepsilon 4} + T_\varepsilon + \Pi_\varepsilon + D_\varepsilon - \Gamma \tag{5}$$

The definition and the role of indivisual terms on the right-hand side of Eq. (5) are given in Rodi and Mansour(1993). To solve this equation, physical modeling is required for many unknown terms. Similar to the usual LRN models, Nagano and Shimada(1993) recently modeled the production terms, $P_{\varepsilon 1}$, $P_{\varepsilon 2}$, $P_{\varepsilon 3}$, $P_{\varepsilon 4}$, and destruction term, Γ, of dissipation equation altogether. They also modeled the turbulent diffusion term, T_ε, and the pressure diffusion term, Π_ε, which were ignored in the previous LRN models. However, their model lacks the ability to account for individual production term effects and includes a rather empirical and complex damping function.

The new model for Eq. (5) retains the basic modeling of $P_{\varepsilon 4}$ and Γ similar to the previous LRN models because they are mainly dominant in the turbulent region and have little effect in the low Reynolds number region. The terms of $P_{\varepsilon 4}$ and Γ are given as follows.

$$P_{\varepsilon 4} = C_{\varepsilon 1}\frac{\varepsilon}{k}P_k \tag{6}$$

$$\Gamma = C_{\varepsilon 2} f_2 \frac{\varepsilon^2}{k} \tag{7}$$

In Eqs. (6)-(7), the model constants $C_{\varepsilon 1}$ and $C_{\varepsilon 2}$ are 1.45 and 1.90, respectively, as in the previous LRN models. The damping function, f_2, is to be given in section 2.2.3. However, Eqs. (6)-(7) are assumed for isotropic turbulent flows. In an anisotropic flow near the wall, their predictions show discrepancy with the DNS data as Rodi and Mansour(1993) pointed out. Therefore, Eq. (6)-(7) may require an additional destruction term, ξ, to account for anisotropic production effect near the wall. The final form of dissipation rate equation becomes

$$\frac{D\varepsilon}{Dt} = C_{\varepsilon 1}P_k\frac{\varepsilon}{k} - C_{\varepsilon 2}f_2\frac{\varepsilon^2}{k} + \xi + P_{\varepsilon 1} + P_{\varepsilon 2} + P_{\varepsilon 3} + T_\varepsilon + \Pi_\varepsilon + D_\varepsilon \tag{8}$$

2.2 Modeling of ε equation

2.2.1 Modeling of $P_{\varepsilon 1}$, $P_{\varepsilon 2}$

Applying the order of magnitude analysis of Tennekes and Lumley(1972), the ratio of production terms can be written as

$$\frac{P_{\varepsilon 1} + P_{\varepsilon 2}}{P_{\varepsilon 4}} = O\left[\frac{S}{(\varepsilon/\nu)^{1/2}}\frac{1}{\mathrm{Re}_t^{1/2}}\right] \tag{9}$$

Using Eq. (6), $P_{\varepsilon 1} + P_{\varepsilon 2}$ can be modeled as

$$P_{\varepsilon 1} + P_{\varepsilon 2} = C_{\varepsilon 1} f_\beta C'_\beta \beta \frac{\varepsilon}{k} P_k \tag{10}$$

where C'_β is model constant, f_β is a new damping function representing $1/\mathrm{Re}_t^{1/2}$, and β is the ratio of the mean field time scale S to the turbulent field time scale $(\varepsilon/\nu)^{1/2}$. For a fully developed flow, β becomes

$$\beta = \frac{S}{(\varepsilon/\nu)^{1/2}} = \frac{|dU/dy|}{(\varepsilon/\nu)^{1/2}} \tag{11}$$

The model constant C'_β can be determined by considering asymptotic behaviors of β, k, ε, and P_k near the wall. According to Chapman and Kuhn(1986), these terms can be expanded as functions of non-dimensional distance from the wall, y^+, as

$$U^+ = U/u_\tau = y^+ + \cdots \tag{12a}$$

$$k^+ = k/u_\tau^2 = a_k y^{+2} + b_k y^{+3} + \cdots \tag{12b}$$

$$\varepsilon^+ = \varepsilon/u_\tau^4\nu = 2a_k + 4b_k y^+ + \cdots \tag{12c}$$

$$\overline{uv}^+ = \overline{uv}/u_\tau^2 = a_{uv} y^{+3} + b_{uv} y^{+4} + \cdots \tag{12d}$$

where a_k, b_k, a_{uv} and b_{uv} are constants.

P_k is defined as

$$P_k^+ = \frac{P_k}{u_\tau^4/\nu} = \overline{uv}^+\frac{dU^+}{dy^+} = a_{uv} y^{+3} + \cdots \tag{13}$$

Substituting Eqs. (12) and (13) back into Eq. (10) yields the following limiting behavior of $P_{\varepsilon 1}^+ + P_{\varepsilon 2}^+$ near the wall.

$$P_{\varepsilon 1}^+ + P_{\varepsilon 2}^+ = C'_\beta \beta f_\beta C_{\varepsilon 1}(2a_{uv} y^+ + O(y^{+2})) \tag{14}$$

Meanwhile, the exact $P_{\varepsilon 1}^+ + P_{\varepsilon 2}^+$ can be written as a function of fluctuating velocities, using Taylor series expansion, as Mansour *et al.* (1988) suggested.

$$P_{\varepsilon 1}^{+}+P_{\varepsilon 2}^{+}=4a_{uv}y^{+}+4Cy^{+2}+O(y^{+3}) \quad (15)$$

Though Eqs. (14) and (15) represent two different forms of $P_{\varepsilon 1}^{+}+P_{\varepsilon 2}^{+}$, coefficients of the corresponding terms should be identical to each other. A comparison of coefficients of the largest terms gives

$$C_{\varepsilon 1}C_{\beta}'\beta f_{\beta}=2 \quad (16)$$

Here, f_{β} represents $1/\mathrm{Re}_t^{1/2}$ which becomes zero away from the wall and can be approximated as

$$f_{\beta}=\exp[-(\mathrm{Re}_t/C_{f\beta})^2] \quad (17)$$

The value of $C_{f\beta}$ of Eq. (17) is determined to be 120 from the condition that f_{β} must be zero beyond the logarithmic layer and the use of the Re_t value from DNS data at $\mathrm{Re}_\tau=395$ (Mansour *et al.*, 1988). Also, β at the wall can be evaluated from Eqs. (11) and (12d) to be

$$\beta=\frac{|dU^{+}/dy^{+}|}{\varepsilon^{+1/2}}=\frac{1}{\sqrt{2a_k}}=\frac{1}{\sqrt{\varepsilon_w^{+}}} \quad (18)$$

Thus, β at the wall depends on the wall dissipation rate, $\varepsilon_w^{+}=2a_k$, which can be obtained from DNS data. Mansour *et al.* (1988) reported that ε_w^{+} is about 0.22081 for $\mathrm{Re}_\tau=395$. Now, the model constant C_{β}' of Eq. (16) can be found by substituting $C_{\varepsilon 1}$, f_{β} and β values into Eq. (16). The resulting value of C_{β}' is about 0.65. The final form is

$$P_{\varepsilon 1}+P_{\varepsilon 2}=0.65\cdot C_{\varepsilon 1}\beta\frac{\varepsilon}{k}P_k\exp[-(\mathrm{Re}_t/120)^2] \quad (19)$$

2.2.2 Modeling of a additional destruction term in dissipation rate equation

Rodi (1971) derived the ε equation for isotropic flows. The ε equation, however, requires modification for the near-wall flow since this flow is anisotropic. As suggested in Eq. (8), the additional destruction term, ξ, is introduced in this study. For anisotropic turbulent flow, the spectral energy equation (Hinze, 1959) is

$$\frac{\partial}{\partial t}E(\kappa,t)+\gamma(\kappa,t)\frac{dU}{dy}=F(\kappa,t)-2\nu\kappa^2E(\kappa,t) \quad (20)$$

(turbulent production by the mean motion; dissipation rate)

Here, E is the energy spectrum, F is the transfer spectrum, κ is the wavenumber and γ is defined as follow,

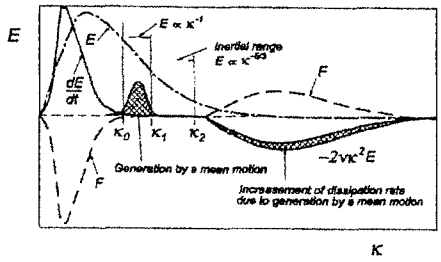

Fig. 1 Spectrum E and spectral energy balance at a near-wall region.

$$\gamma=2\pi\kappa^2\left[2(E_{1,2})_{a\nu}-\left(\kappa_1\frac{\partial E_{i,i}}{\partial\kappa_2}\right)_{a\nu}\right] \quad (21)$$

where $E_{i,i}$ is a spectrum tensor of turbulence kinetic energy and κ_i is the component of wavenumber vector. The budget of Eq. (20) is shown in Fig. 1.

In Fig. 1, the hatched regions represent additional production and dissipation rate by the mean motion due to anisotropy. According to Hinze (1959) this additional production energy is directly delivered to the small scale turbulence flow by the mean motion, instead of transfer spectrum, when the vorticity of the mean motion is comparable with that of the turbulence flow. So, the transfer spectrum F remains unchanged for both isotropic and anisotropic flows. The additional turbulence production must increase the dissipation rate as shown in Fig. 1.

With the definition of $\varepsilon=2\nu\int_0^{\infty}\kappa^2E d\kappa$, Eq. (20) can be integrated from $\kappa=0$ to $\kappa=\infty$ to yield the ε equation for anisotropic flow.

$$\frac{d\varepsilon}{dt}=2\nu\int_0^{\infty}\kappa^2F d\kappa-4\nu^2\int_0^{\infty}\kappa^4E d\kappa-2\nu\frac{dU}{dy}\int_0^{\infty}\kappa^2\gamma d\kappa \quad (22)$$

(ε destruction; additional ε production)

Eq. (22) is rearranged as

$$\frac{d\varepsilon}{dt}=2\nu\int_0^{\kappa_1}\kappa^2F d\kappa-\underbrace{2\nu\int_{\kappa_2}^{\infty}(2\nu\kappa^4E-\kappa^2F)\,d\kappa}_{D}-\underbrace{2\nu\frac{dU}{dy}\int_0^{\infty}\kappa^2\gamma d\kappa}_{G} \quad (23)$$

The first term of Eq. (23) is modelled by Rodi (1971) as

$$2\nu\int_0^{\kappa 1}\kappa^2 F d\kappa = C_{\varepsilon 1}\frac{\varepsilon}{k}P_k - C_{\varepsilon 2}\frac{\varepsilon^2}{k} \tag{24}$$

Unlike Rodi(1971)'s ε equation, additional terms due to anisotropic flow are appeared in Eq. (23) near the wall. G' is the additional production of ε. Since the contribution of G' to the ε equation is the same as that of $P_{\varepsilon 1}$ and $P_{\varepsilon 2}$, Eq. (19) can be used as the modeling form of this term. Meanwhile, D' is an additional destruction proportional to G' near the wall and this term is modelled as follows.

From the correlation of spectral energy, G' is found to be

$$G' = -2\nu\frac{dU}{dy}\int_0^{\infty}\kappa^2\gamma d\kappa = -4\pi\nu\frac{dU}{dy}\int_0^{\infty}\kappa^4 (E_{1,2})_{av} d\kappa$$
$$= 2\nu\overline{\frac{\partial u}{\partial x_i}}\,\overline{\frac{\partial v}{\partial x_i}}\frac{dU}{dy} \tag{25}$$

where the integration of the second term of γ in Eq. (21) is zero from the spectrum relation (Hinze, 1959).

Since the D' term, named by ξ hereafter, is proportional to the G' term, ξ is assumed to be the form multiplying Eq. (25) by a model constant C_ξ.

$$\xi = -C_\xi 2\nu\overline{\frac{\partial u}{\partial x_i}}\,\overline{\frac{\partial v}{\partial x_i}}\frac{dU}{dy} \tag{26}$$

Now, ξ is expressed as product of dissipation rate tensor and mean velocity gradient. Since no dissipation rate tensor can be found in the k-ε model, ξ is rewritten by using the pseudo dissipation rate, $\tilde{\varepsilon}$, which becomes zero at the wall. And the absolute value of mean velocity gradient, dU/dy is taken so that ξ is always negative.

$$\xi = -C_\xi\tilde{\varepsilon}\left|\frac{dU}{dy}\right| \tag{27}$$

To determine, C_ξ, a numerical simulation is performed by changing the values of C_ξ for the best fit against the DNS data. The optimum value of C_ξ is found to be 0.35.

In addition to the model constant, a damping function is further introduced to ensure that the additional ε destruction disappears in the logarithmic layer. The additional ε destruction distribution should follow the additional ε production distribution to maintain energy balance. Therefore, the new damping function can be set to be

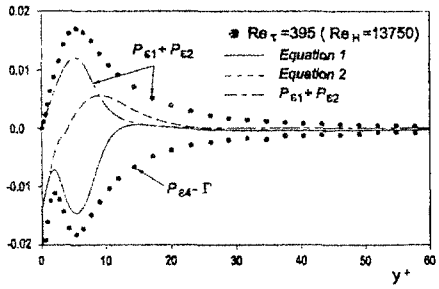

(a) Distribution of $P_{\varepsilon 1}+P_{\varepsilon 2}$ and $P_{\varepsilon 4}-\Gamma$

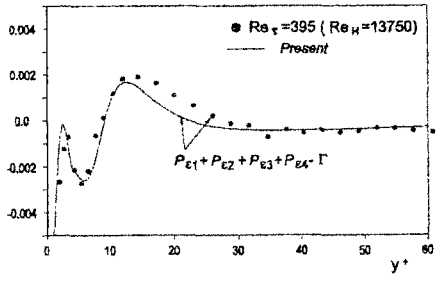

(b) Distribution of $P_{\varepsilon 1}+P_{\varepsilon 2}+P_{\varepsilon 3}+P_{\varepsilon 4}-\Gamma$

Fig. 2 Comparison of the budget of ε equation. (Equation 1 : $C_{\varepsilon 1}\frac{\varepsilon}{k}P_k - f_2 C_{\varepsilon 2}\frac{\varepsilon^2}{k} - 0.35\tilde{\varepsilon}\frac{dU}{dy}$, Equation 2 : $C_{\varepsilon 1}\frac{\varepsilon}{k}P_k - f_2 C_{\varepsilon 2}\frac{\varepsilon^2}{k}$)

equivalent to f_β of Eq. (17). Including the model constant and the damping function, the final form of ξ model can be written as

$$\xi = -0.35\tilde{\varepsilon}\left|\frac{dU}{dy}\right|\exp\left[-\left(\frac{\mathrm{Re}_t}{120}\right)^2\right] \tag{28}$$

In Fig. 2, the distributions of $P_{\varepsilon 4}-\Gamma$ from the present model and Rodi(1971)'s model are shown with $P_{\varepsilon 1}+P_{\varepsilon 2}$. The present model predicts the DNS data trend at $y^+<10$ while the Rodi(1971)'s model doesn't. Especially, the sum of $P_{\varepsilon 1}+P_{\varepsilon 2}+P_{\varepsilon 3}+P_{\varepsilon 4}-\Gamma$ of present model agrees with the DNS data. From this result, it is seen that the modelling of near-wall terms, $P_{\varepsilon 1}+P_{\varepsilon 2}$ and ξ are successfully perfomed.

2.2.3 Modeling of other terms

The gradient production, $P_{\varepsilon 3}$, has a near wall distribution different from those of the other production terms. This indicates that $P_{\varepsilon 3}$ requires a separate modeling approach. Rodi and Mansour(1993), Nagano and Shimada(1993), and

Shin and Choi(1996) proposed their own $P_{\varepsilon 3}$ models. Rodi and Mansour(1993)'s model shows correct trends for the ε distribution. However, it overpredicts the maximum and minimum values of dissipation rate. Other models are generally too complex to use. Therefore, the $P_{\varepsilon 3}$ of Rodi and Mansour(1993) is employed after multiplying 0.8 to adjust for its overprediction.

The damping function f_2 for ε destruction in Eq. (7) is adopted from the work of Nagano and Tagawa(1990).

$$f_2=[1-0.3\exp[-(\mathrm{Re}_t/6.5)^2]][1-\exp(-y^+/6)]^2 \quad (29)$$

Since the turbulent diffusion, T_ϕ, and the pressure diffusion. Π_ϕ, are not negligible near the wall, these terms should also be included in the ε equation as well. The turbulent diffusion model of Nagano and Shimada(1993) shows good performance; however, it decreases slowly near the wall. The model of Nagano and Shimada(1993) is used in this study after modifying the exponent of σ_k from 0.75 to 1.0 as shown in Eq. (45a). The pressure diffusion model is also adopted from Nagano and Shimada(1993) as it has shown a good agreement with DNS data.

2.3 Eddy viscosity damping function

The damping function, f_μ, of Eq. (3) is known to be important to ensure correct near wall behavior of mean velocity and turbulent viscosity. Myong(1988) and Nagano and Tagawa(1990) modeled the f_μ function on physical basis. However, their prediction has some discrepancy when compared to the channal flows DNS data. Since the f_μ functions of the LRN models have similar problems, a new f_μ function is proposed to correct for this shortcoming. From dimensional analysis, the turbulent viscosity can be written as

$$\nu_t=C_{eddy}\sqrt{k}L_d f_d \quad (30)$$

where f_d is the damping function and C_{eddy} is a model constant. L_d represents the length scale of dissipation rate which becomes L_{dh} in the high Reynolds number region and L_{dl} in the low Reynolds number region. In general, the length scale of dissipation rate in the high Reynolds number region can be approximated as

$$L_{dh}=C_{dh}k^{3/2}/\varepsilon \quad (31)$$

Meanwhile, L_{dl} has been proposed in various forms. The length scale, $\sqrt{\nu k/\varepsilon}$ of Myong(1988) and the Kolmogorov length scale $\eta=(\nu^3/\varepsilon)^{1/4}$ of Nagano and Tagawa(1990) are good examples of L_{dl}. Considering its small value very near the wall($y^+\leq 2\sim 3$), η may be used as L_{dl} in this region. Away from the wall($y^+\geq 2\sim 3$), $\sqrt{\nu k/\varepsilon}$ could represent L_{dl} reasonably. L_{dl} is, therefore, proposed to include these trends by combining η and $\sqrt{\nu k/\varepsilon}$ with hyperbolic tangent function.

$$L_{dl}=C'_{dl}\sqrt{\frac{\nu k}{\varepsilon}}\frac{1}{\tanh(\mathrm{Re}_t^{1/4}/C_{dl})} \quad (32)$$

Now, the length scale, L_d, can be obtained from L_{dl} and L_{dh}. Myong(1988) suggests L_d as a summation of L_{dl} and L_{dh}. However, the simple summation of Eq. (31) and (32) does not ensure the correct length scale transition for different flow regions. Therefore, a fourth order interpolation is applied to have the final form of length scale, L_d.

$$L_d=(L_{dl}^4+L_{dh}^4)^{1/4} \quad (33)$$

And this equation is arranged with respect to $L_{dh}(=k^{3/2}/\varepsilon)$.

$$L_d=\frac{k^{3/2}}{\varepsilon}\left[\left(\frac{C_1}{\mathrm{Re}_t^{1/2}}\frac{1}{\tanh(\mathrm{Re}_t^{1/4}/C_{dl})}\right)^4+1\right)\Bigg]^{1/4} \quad (33a)$$

It is verified from DNS data that L_d of Eq. (33a) becomes to L_{dh} as Re_t proportial to y^+ becomes large. Utilizing Eqs. (33a), (30) and (3), f_μ function can be obtained.

$$f_\mu=\left[\left(\frac{C_1}{\mathrm{Re}_t^{1/2}}\frac{1}{\tanh(\mathrm{Re}_t^{1/4}/C_{dl})}\right)^4+1\right]^{1/4}\cdot f_d \quad (34)$$

The damping function, f_d, can be found by considering the distribution of turbulent properties near the wall. From Eq. (12), following relationships can be obtained at the wall.

$$\nu_t^+=\frac{\overline{uv}}{dU/dy}\propto y^{+3},\quad k^+\propto y^{+2},\quad \varepsilon^+\approx\varepsilon_w^+ \quad (35)$$

From Eqs. (35) and (3), the near wall behavior of f_μ is found to be proportional to $1/y^+$. Since the term in the square bracket of Eq. (34) follows $1/y^{+3}$ distribution, f_d function must be proportional to y^{+2} to satisfy the limiting behavior of f_μ. Now, f_d can be

$$f_d=1-\exp[-(y^+/C_{fd})^2] \tag{36}$$

where C_{fd} is the model constant. C_{fd} could be set to 41 to satisfy the condition that f_d must be one beyond the logarithmic layer.

C_1 and C_{d1} can be determined from the asymptotic analysis of turbulent properties. From Eq. (3), (12) and Boussinesq approximation for $\overline{u_iu_j}$, the near wall behavior of f_μ can be found.

$$f_\mu=\frac{\varepsilon^+\overline{uv}^+}{C_\mu k^{+2}dU^+/dy^+}=\frac{2a_k\cdot a_{uv}}{C_\mu a_k^2}\frac{1}{y^+}+\cdots \tag{37}$$

On the other hand, the near wall behavior of f_μ can also be obtained directly from Eq. (34) together with Eq. (36) and the limiting behavior of Re_t.

$$f_\mu=\frac{C_1\cdot C_{d1}}{\mathrm{Re}_t^{3/4}}\frac{y^{+2}}{C_{fd}^2}+\cdots=\frac{C_1\cdot C_{d1}}{C_{fd}^2}\left(\frac{2}{a_k}\right)^{3/4}\frac{1}{y^+}+\cdots \tag{38}$$

From Eqs. (37) and (38), the model constant, $C_1\cdot C_{d1}$ is obtained as follows.

$$C_1\cdot C_{d1}=\frac{2a_k\cdot a_{uv}}{C_\mu a_k^2}C_{fd}^2\left(\frac{a_k}{2}\right)^{3/4} \tag{39}$$

Inserting DNS data at $\mathrm{Re}_\tau=395$ into Eq. (39), $C_1\cdot C_{d1}$ is found to be 35. However, the values of the wall dissipation, ε_w^+, and a_{uv} vary with Re_δ, C_1 and C_{d1} can be further refined after including the effect of Reynolds number.

2.4 The Reynolds number effect

Recently developed LRN models can accurately predict high Reynolds number flows. However, their predictions are poor for low Reynolds number flows. The current model takes into account this Reynolds number effect.

$C_1\cdot C_{d1}$ of f_μ is obtained from DNS data and shows Reynolds number dependence in Fig. 3. $C_1\cdot C_{d1}$ can be curve-fitted as follows.

$$C_1\cdot C_{d1}=40\cdot f_{\mathrm{Re}} \tag{40}$$

$$f_{\mathrm{Re}}=1-0.5\exp(-\mathrm{Re}_\delta/10^4) \tag{40a}$$

Since Eq. (40) is the form of multipling C_1 and C_{d1} together, C_1 and C_{d1} must be divided. C_1 is experientially determined as 4.0 from the fact that a constant similar to C_1 of the present model has a value between 3.5 and 4.0 in Myong(1988) and Nagano and Tagawa(1990). Thus,

$$C_1=4.0,\ C_{d1}=10\cdot f_{\mathrm{Re}} \tag{41}$$

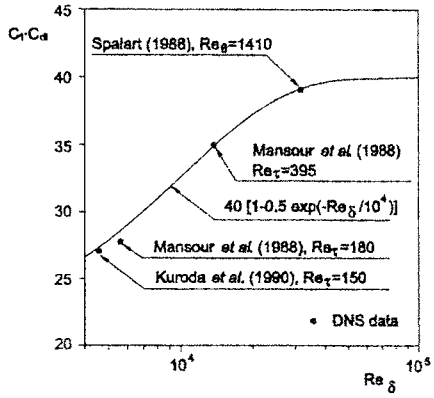

Fig. 3 $C_1\cdot C_{d1}$ distribution with respect to Re_δ.

Table 1 Constant variation with Re_δ

Re_δ	C_1	C_{d1}	$C_{f\beta}$	$C_{f\sigma}$
13750	3.5	10	120	100
For all of Re_δ	4.0	$10f_{\mathrm{Re}}$	$140f_{\mathrm{Re}}$	$120f_{\mathrm{Re}}$

The damping functions of Eqs. (17) and (28) should depend on Re_t and the mean flow Reynolds number Re_δ for the following reasons. According to the DNS data, limiting behavior of Re_t near the wall depends on ε_w^+ which varies with Re_δ. ε_w^+ decreases as Re_δ decreases and Re_t eventually also decreases. In other words, Re_t should be decreased as Re_δ decreases, and, consequently, the damping effects of Eqs. (17) and (28) should increase. Therefore, the model constants of these damping functions should be corrected by Eq. (40a) to include the Re_δ effect. The values of the current model constants for the damping functions are determined from the DNS data for $\mathrm{Re}_\tau=395$. Incorporating the Re_δ effects on the damping function, the revised model constants are shown in Table 1.

2.5 Final form of proposed LRN model

Substituting each modeled term into the governing equations, the final form of newly proposed low Reynolds number $k-\varepsilon$ model are presented belows.

Turbulent kinetic energy equation

$$\frac{Dk}{Dt}=\left[\left(\nu+\frac{\nu_t}{\sigma_k}\right)k_{,y}\right]_{,y}+P_k-\varepsilon-0.5\left[\nu f_{wk}\frac{k}{\varepsilon}\varepsilon_{,y}\right]_{,y} \tag{42}$$

Dissipation rate equation

$$\frac{D\varepsilon}{Dt}=\left[\left(\nu+\frac{\nu_t}{\sigma_\varepsilon}\right)\varepsilon_{,y}\right]_{,y}+C'_{\varepsilon 1}P_k\frac{\varepsilon}{k}-C_{\varepsilon 2}f_2\frac{\varepsilon^2}{k}$$
$$-0.35\cdot\tilde{\varepsilon}\left|\frac{dU}{dy}\right|f_\beta$$
$$+0.5\cdot\left[\nu\frac{\varepsilon}{k}f_{wk}(1-f_{wk})k_{,y}\right]_{,y}$$
$$+0.8\cdot\left[\nu\nu_t(U_{,yy})^2+0.006\nu\frac{k}{\varepsilon}k_{,y}U_{,y}U_{,yy}\right] \quad (43)$$

f_μ function

$$f_\mu=\left[\left(\frac{4.0}{\mathrm{Re}_t^{1/2}}\frac{1}{\tanh(\mathrm{Re}_t^{1/4}/C_{d1})}\right)^4+1\right]^{1/4}\cdot\left[1-\exp\left[-\left(\frac{y^+}{41}\right)^2\right]\right] \quad (44)$$

Here, the other damping functions and model constants are also given by

$$\sigma_k=\frac{1.2}{1+3.5\exp[-(\mathrm{Re}_t/C_{f\sigma})]} \quad (45a)$$

$$\sigma_\varepsilon=\frac{1.3}{1.2}\sigma_k \quad (45b)$$

$$C'_{\varepsilon 1}=1.45\cdot(1+0.65f_\beta\beta) \quad (45c)$$

$$\beta=|dU/dy|/(\varepsilon/\nu)^{0.5} \quad (45d)$$

$$f_\beta=\exp|-(\mathrm{Re}_t/C_{f\beta})^2] \quad (17)$$

$$f_{\mathrm{Re}}=1-0.5\exp(-\mathrm{Re}_\beta/10^4) \quad (40a)$$

$$f_{wk}=\exp[-(y^+/9)^2] \quad (46)$$

and the model constants $C_{f\beta}$, $C_{f\sigma}$, C_{d1} are shown in Table 1.

3. Numerical Method

The governing equations for fully developed turbulent flow are discretized by finite volume method (FVM), and the discretized equations are solved by TDMA. The symmetric boundary condition is used at the centerline and no-slip, no-penetration conditions with $k=0$ and $\varepsilon_w=\nu(\partial^2k/\partial y^2)_w$ are applied at the wall. Since ε_w is given in the form of a second spatial derivative, it often induces the numerical instability. As a remedy, Chapman and Kuhn (1986)'s relationship is applied (Eq. (47)).

$$\varepsilon_w=\frac{4\nu k_1}{y_1^2}-\varepsilon_1 \quad (47)$$

where the subscript 1 denotes the first grid point from the wall. To assure the numerical accuracy, we set the first grid point at $y_1^+=0.1$, and a non-uniform grid is generated with an increasing ratio of 1.01. Grid independence test is performed against different number of grid points and the grid independence is achieved for a total grid number above 65.

4. Results and Discussion

4.1 Evaluation of the modified model

The performance of the new LRN model is compared with the corresponding DNS data and the model of Nagano and Tagawa(1990). As shown in Table 2, test cases are selected by combining new and existing models. The 'Present' case refers to using Eqs. (43) and (44) for the dissipation rate equation and the damping function. Case A uses the new damping function, Eq. (44) and the dissipation rate equation of Nagano and Tagawa(1990). Case B is setup with the damping function of Nagano and Tagawa(1990) and the newly proposed dissipation rate equation. Thus, the new dissipation rate and damping function models can be evaluated individually. The effects of model constant correction are assessed via Case C and Case D which include different sets of model constants as shown in Table 2. Fig. 4(a) presents the near wall behavior of ε^+. Present case and Case B produce better predictions than the Case A. Thus the new dissipation rate

Table 2 List of test case

Case	f_μ	ε equation	C_1	C_{d1}	$C_{f\beta}$	$C_{f\sigma}$
Present	Eq. (44)	Eq. (43)	4.0	$10f_{\mathrm{Re}}$	$140f_{\mathrm{Re}}$	$120f_{\mathrm{Re}}$
Case A	Eq. (44)	NT's model	4.0	$10f_{\mathrm{Re}}$	$140f_{\mathrm{Re}}$	$120f_{\mathrm{Re}}$
Case B	NT's model	Eq. (43)	4.0	$10f_{\mathrm{Re}}$	$140f_{\mathrm{Re}}$	$120f_{\mathrm{Re}}$
Case C	Eq. (44)	Eq. (43)	3.5	10	120	100
Case D	Eq. (44)	Eq. (43)	4.0	$10f_{\mathrm{Re}}$	120	100

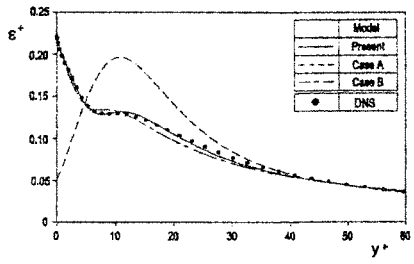

(a) Dissipation rates

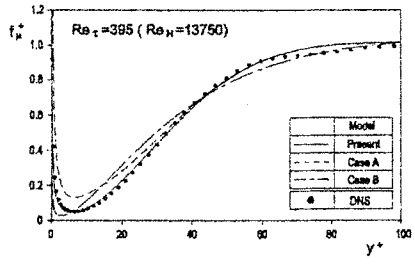

(b) Damping functions

Fig. 4 Evaluation of the modified ε equation and f_μ function(● : Mansour et al., 1988).

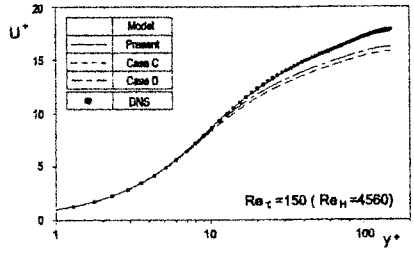

(a) Mean velocities

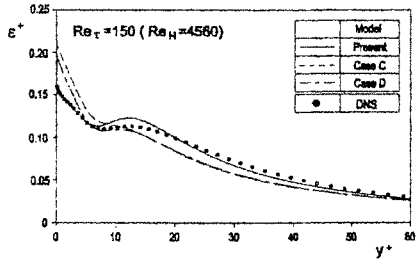

(b) Dissipation rates

Fig. 5 Verification of Reynolds effect correction (● : Kuroda *et al.*, 1990).

equation model can describe near wall behavior of ε^+. Present case results closely follow the DNS data for ε^+ while Case B's results show deviations from the DNS data. The effect of damping function model is displayed more clearly in Fig. 4(b). Fig. 5 shows the predictions for Re_τ=150. Comparisons of U^+ and ε^+ clearly show that the Present case results are in excellent agreement with the DNS data (Kuroda *et al.*, 1990). Thus, one can infer that the proposed model properly reflects the Reynolds number effect.

4.2 Turbulent channel flow

Performance of the current model is verified against fully developed turbulent channel flows of different Reynolds numbers. For comparison, prediction results from the models of Nagano and Tagawa(1990), Nagano and Shimada(1993) and Shin and Choi (1996) are also presented in Fig. 6. Acceptable agreement between predictions and the corresponding DNS data (Mansour *et al.*, 1988) is found for mean velocity, U^+, and turbulent kinetic energy, k^+. Present case, however, shows the best agreement, and the same trend can be seen for the dissipation rate, ε^+, as explained in previous section. The budget of k^+ equation also shows excellent agreement with DNS data (Mansour *et al.*, 1988).

In Fig. 7, the predictions for different Reynolds number are presented. Similar to the case of Re_τ =395, the current model can predict the DNS data(Kuroda *et al.*, 1990) except that slightly overpredicted k^+ is observed near center region. Therefore, the current model successfully accounts for the Reynolds number effect(Fig. 8).

4.3 Turbulent pipe flow

The model is applied to a fully developed turbulent pipe flow. Fig. 9 shows predictions from different models and the experimental data of Schildknecht *et al.* (1979) for Re_τ=500.

General agreement is observed for U^+ and k^+ except near center line of pipe. Predictions for ε^+ shows a similar agreement between predictions from the current model and the Nagano and Shimada(1993) model with the trend in channel flows. The visible discrepancy between the model predictions and the experimental data is well known and is thought to be due to measurement errors. A similar comparison against Laufer

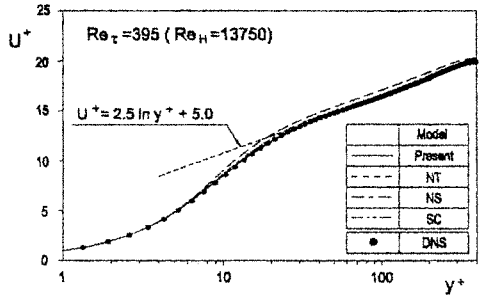

(a) Mean velocities

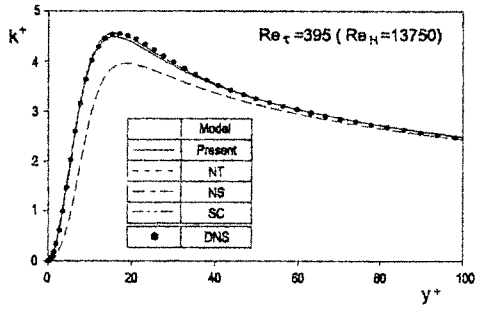

(b) Turbulent kinetic energies

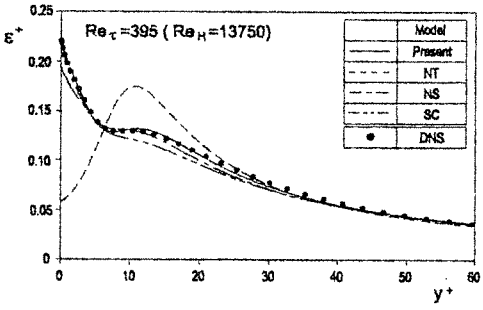

(c) Dissipation rates

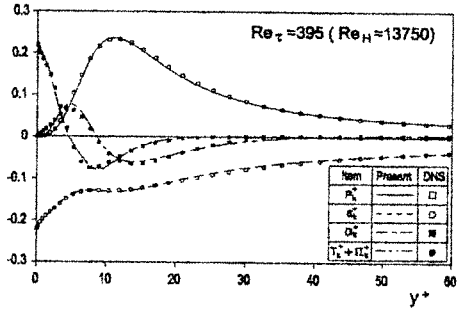

(d) Budget of turbulent kinetic energies

Fig. 6 Comparison of prediction results in a channel flow for $Re_\tau = 395$ (● : Mansour *et al.*, 1988).

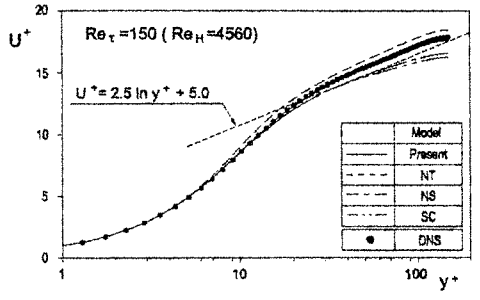

(a) Mean velocities

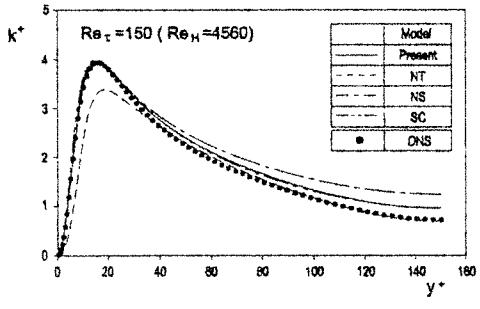

(b) Turbulent kinetic energies

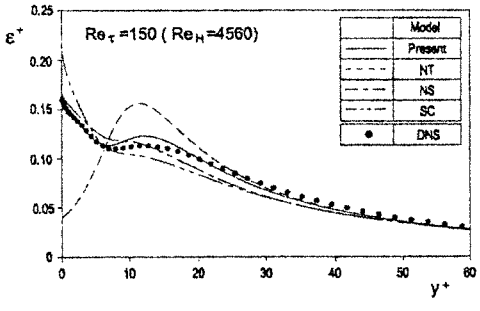

(c) Dissipation rates

Fig. 7 Comparison of prediction results in a channel flow for $Re_\tau = 150$ (● : Kuroda *et al.*, 1990).

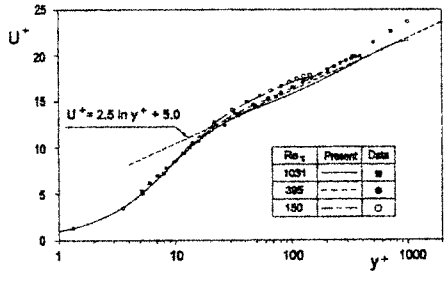

Fig. 8 Mean velocity distributions in channel flows with various Reynolds number. (■ : Johanson and Alfredson (1982), ● : Mansour *et al.* (1988), ○ : Kuroda *et al.* (1990).

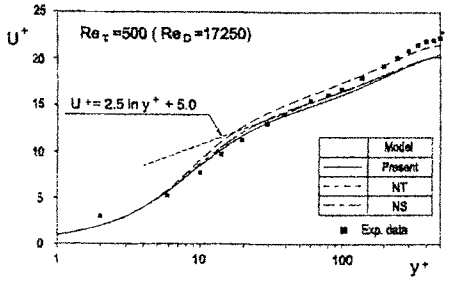

(a) Mean velocities

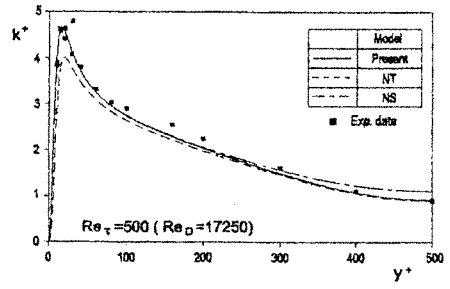

(b) Turbulent kinetic energies

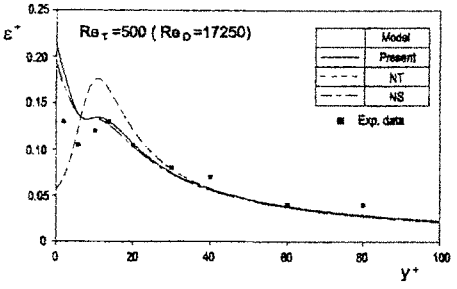

(c) Dissipation rates

Fig. 9 Comparsion of prediction results in a pipe flow for $Re_\tau = 500$(■ : Schildknecht *et al.*, 1979).

(1954)'s experimental data is shown in Fig. 10

Fig. 11 also presents comparison results of U^+ prediction at different Reynolds numbers. The good agreement between predictions and data confirms that the current model can correctly predict turbulent flows at various Reynolds numbers.

4.4 Turbulent flat-plate flow

The model is also applied to turbulent flat-plate flow cases. The predictions are compared with the DNS data of Spalart(1988) and the experimental data of Nagano *et al.* (1991) (Fig. 12).

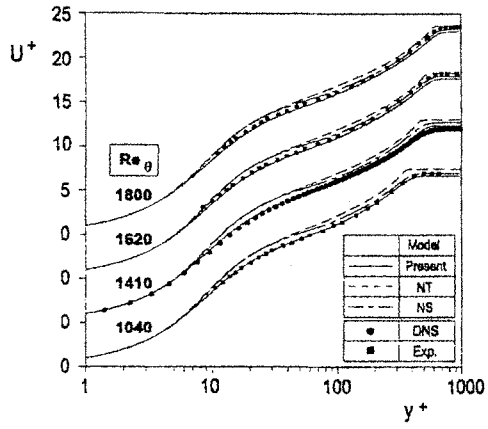

(a) Mean velocities

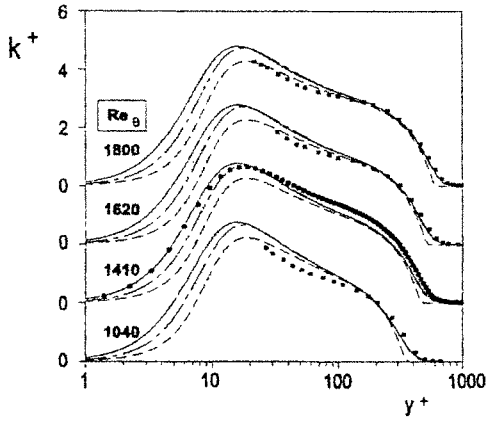

(b) Turbulent kinetic energies

Fig. 10 Comparison of prediction results in a pipe flow for $Re_\tau = 1052$(■ : Laufer. 1954).

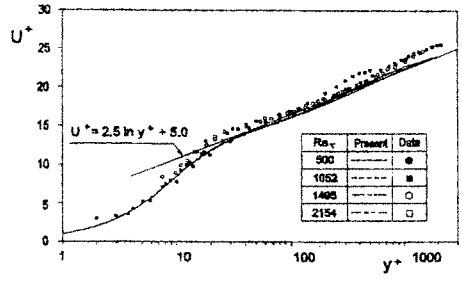

Fig. 11 Mean velocity distributions in pipe flows with various Reynolds number.(● : Schildknecht *et al.* (1979), ■ : Laufer(1954), ○, □ : Hishida *et al.* (1976)).

Again, the present U^+ model can predict more accurately than any other model. k^+ predicted by

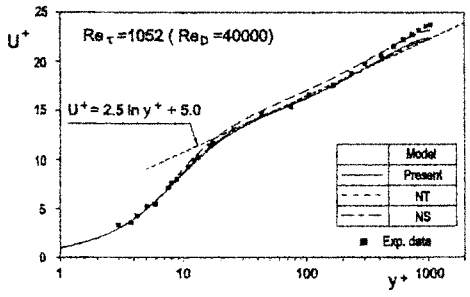

(a) Mean velocities

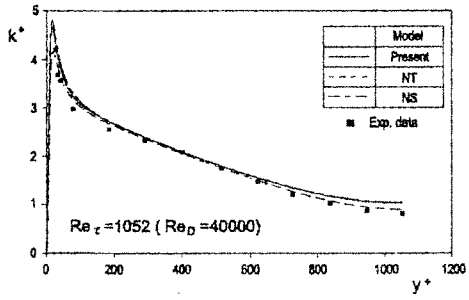

(b) Turbulent kinetic energies

Fig. 12 Mean velocity and turbulent kinetic energy distributions in flat plate flows(■ : Nagano *et al.*(1991), ● : Spalart(1988)).

the current model also agrees well with the DNS data, but shows a slight discrepancy with the experimental data. From this comparison, the current model is shown to be capable of predicting boundary layer flow.

5. Conclusions

A new $k-\varepsilon$ model has been developed based on physical consideration of the near wall behavior of turbulence quantities. In the new $k-\varepsilon$ model, the dissipation rate equation and the damping function are improved. The present model has been verified against the DNS and experimental data for internal and external flows for a wide range of Reynolds numbers. The present model can accurately predict the turbulence field including mean velocity, kinetic energy and its dissipation rate. Particularly, the proposed model with the improved ε equation clearly shows its ability to reproduce the ε distribution which has its maximum value at the wall and then decreases away from the wall. Also, the Reynolds number effect is adequately reflected in the proposed model to yield excellent predictions for flows at different Reynolds numbers.

References

Chapman, D. R. and Kuhn, G. D., 1986, "The Limiting Behaviour of Turbulence Near a Wall," *J. Fluid Mechanics*, Vol. 170, pp. 265~292

Hanjalic, K. and Launder, B. E., 1976, "Contribution Towards a Reynolds Stress Closure for Low Reynolds Number Turbulence," *J. Fluid Mechanics*, Vol. 94, pp. 593~610

Hinze, J. O., 1959, *Turbulence*, McGRAW-HILL, New York

Hishida, M., Nagano, Y. and Kobayashi, M., 1976, "Turbulent Boundary Layer in the Entrance Region of a Pipe (1st Report, Velocity Profile and Wall Shear Stress)," *Trans. JSME*, Vol. 42, pp. 1794~1802

Johansson, A. V. and Alfredsson, P. H., 1982, "On the Structure of Turbulent Channel Flow," *J. Fluid Mechanics*, Vol. 122, pp. 295~314

Jones, W. P. and Launder, B. E., 1972, "The Prediction of Laminarization with a Two-Equation Model of Turbulence," *Int. J. Heat Mass Transfer*, Vol. 15, pp. 310~314

Kuroda, A., Kasagi, K. and Hirata, M., 1990, "Investigation of Dynamic Effects of the Mean Shear Rate on the Wall Turbulence via Direct Numerical Simulation," *Proceedings of 27th National Heat Transfer Symposium of Japan*, Vol. 1, pp. 46~48

Laufer, J., 1954, "The Structure of Turbulence in Fully Developed Pipe Flow," *NACA Rep. 1174*

Mansour, N. N., Kim, J. and Moin, P., 1988, "Reynolds Stress and Dissipation-Rate Budgets in a Turbulent Channel Flows," *J. Fluid Mechanics*, Vol. 194, pp. 15~44

Myong, H. K., 1988, Fundamental Studies on Two-Equation Turbulence Model for Numerical Predictions of Wall-Bounded Shear Flow and Heat Transfer, Ph. D. Thesis, University of, Tokyo, Japan.

Nagano, Y. and Shimada, M., 1993, "Modeling

the Dissipation-Rate Equation for Wall Shear Flows(Comparison with Direct Simulation Data)," *Trans. JSME (in japanese)*, Vol. 59, pp. 78~85

Nagano, Y. and Tagawa, M., 1990, "An, improved $k-\varepsilon$ Model for Boundary Layer Flows," *J. Fluids Engineering*, Vol. 112, pp. 33~39

Nagano, Y., Tagawa, M. and Tsuji, T., 1991, "Effects of Adverse Pressure Gradients on Mass Flows and Turbulence Statics in a Boundary Layers," *Turbulent Shear Flows 8*, pp. 7~21

Patel, V. C., Rodi, W. and Scheuerer, G., 1985, "Turbulence Models for Near-Wall and Low -Reynolds Number Flows: A review," *AIAA J.*, Vol. 23, pp. 1308~1319

Rodi, W., 1971, "On the Equation Governing the Rate of Turbulent Energy Dissipation," *Report TM/TN/A/14*, Imperial College of Science and Technology, London

Rodi, W. and Mansour, N. N., 1993, "Low Reynolds Number $k-\varepsilon$ Modeling with the Aid of DNS," *J. Fluids Mechanics*, Vol. 250, pp. 509 ~529

Schildknecht, M., Miller, J. A. and Meier, G. E. A., 1979, "The Influence of Suction on the Structure of Turbulence in Fully Developed Pipe Flow," *J. Fluid Mechanics*, Vol. 90, pp. 67~107

Shin, J. K. and Choi, Y. D., 1996, "Development of Multiple Production $k-\varepsilon$ Equation Model in Low Reynolds Number $k-\varepsilon$ Model with the Aid of DNS Data," *Trans. KSME*, Vol. 20, pp. 304~320

Spalart, P. R., 1988, "Direct Simulation of a Turbulent Boundary Layer up to $R_\theta=1410$," *J. Fluid Mechanics*, Vol. 187, pp. 61~98

Tennekes, H. and Lumley, J. L., 1972, *A First Course in Turbulence*, MIT press